HIGH-ORDER METHODS FOR THE SIMULATION OF TRANSITIONAL TO TURBULENT WAKES

LAURENT COUSIN AND RICHARD PASQUETTI *

Abstract. The paper describes the high-order algorithms that we have developed for the simulation of transitional to turbulent 3D wakes in stratified fluids, through the use of Direct Numerical Simulation (DNS) or Large Eddy Simulation (LES), with applications to the wake of a sphere in a thermally stratified liquid and to the wake of a cylinder respectively.

Key words. Spectral methods, direct numerical simulation, large-eddy simulation, wakes, stratified fluids.

AMS subject classifications. 76A60, 76C05, 76D25, 76V05

1. Introduction. Wakes in stratified liquids may give rise to a large diversity of complex phenomena: wake collapse, internal gravity waves (lee-waves, random internal waves), various flow regimes, depending on the geometry of the obstacle, on the fluid characteristics (Prandtl number), on the flow velocity (Reynolds number) and on the stratification intensity characterized by the "Brunt-Väisälä frequency" (Richardson number). The aim of this paper is to describe the high-order algorithms that we have developed to describe such flows, using Direct Numerical Simulation (DNS) or Large Eddy Simulation (LES). It is assumed that the flow is governed by the "Boussinesq equations": In the domain Ω (boundary Γ) and in the time-interval $(0, t_F)$:

$$
\begin{aligned}
&D_t \boldsymbol{u} = -\nabla p - Ri\, T \boldsymbol{g} + \frac{1}{Re}\nabla^2 \boldsymbol{u} \\
&\nabla . \boldsymbol{u} = 0 \\
&D_t T = \frac{1}{Pe}\nabla^2 T \\
&\qquad + \quad I.C. \quad \& \quad B.C.
\end{aligned}
$$

with t: time, $\boldsymbol{u}$: velocity vector, $\boldsymbol{g}$: normalized gravity vector, p : pressure deviation from the hydrostatic one, T : temperature deviation from a mean one, Re, Pe, Ri : Reynolds, Péclet and Richardson numbers ($Pe/Re = Pr$, Pr: Prandtl number) and $D_t = \partial_t + \boldsymbol{u}.\nabla$, material derivative. B.C. and I.C. stand for boundary conditions and initial conditions respectively.

The computational domain Ω is of channel-type, with an obstacle inside. The streamwise x-direction is assumed much larger than the y-cross-flow and z-spanwise directions. The spanwise direction is assumed homogeneous.

The paper is divided in three parts. First, we focus on DNS and describe the numerical method. Second, we go to LES, for which high-order approximations are highly justified since with low-order methods the approximation errors and subgrid scale modeling adjustments may show comparable amplitudes. Third, results obtained for the DNS of the wake of a sphere in a stratified liquid and for the LES of the turbulent wake of a cylinder are presented.

*Richard.Pasquetti@unice.fr, Lab. J.A. Dieudonné, Université de Nice-Sophia Antipolis, 06108 Nice, France

2. Numerical method. Along the streamwise direction one uses a domain decomposition technique and in each sub-domain a Chebyshev / Fourier spectral approximation: The approximation in space makes use in x of S non-overlapping subdomains with conforming meshes, Fourier expansions in z, Chebyshev polynomial approximations in x and y. The solver is parallelized (one subdomain / processor) and vectorial calculation is used in each subdomain. For the modeling of the bluff body, inside the channel, we use a smoothed penalty technique. At the outlet of the channel, soft outflow boundary conditions are needed: We use the $u-\boldsymbol{\omega}$ conditions that we introduced in [7, 8] (u, streamwise component of the velocity, $\boldsymbol{\omega}$, the vorticity). Here we focus on the time-scheme, which makes use of (i) a transport step, based on an OIF (Operator Integration Factor) semi-Lagrangian method, (ii) a diffusion step and (iii) a projection step, with a "unique grid $P_N - P_{N-2}$" approximation.

2.1. Transport step. Let us focus on the momentum equation. A BEQ (backward Euler of order Q) approximation of the material derivative yields:

$$D_t \boldsymbol{u}(t_{n+1}) = \frac{1}{\Delta t}(\alpha_0 \boldsymbol{u}^{n+1} + \sum_{q=1}^{q=Q} \alpha_q \tilde{\boldsymbol{u}}^{n+1-q}) + O\left(\Delta t^Q\right)$$

with $\boldsymbol{u}^{n+1} \approx \boldsymbol{u}(\boldsymbol{x}, t_{n+1})$ and $\tilde{\boldsymbol{u}}^{n+1-q} \approx \boldsymbol{u}(\boldsymbol{\chi}(\boldsymbol{x}, t_{n+1}; t_{n+1-q}), t_{n+1-q})$, where $\boldsymbol{\chi}(\boldsymbol{x}, t_{n+1}; t)$ solves the characteristics equation:

$$\begin{aligned} \frac{d\boldsymbol{\chi}(\boldsymbol{x}, t_{n+1}; t)}{dt} &= \boldsymbol{u}(\boldsymbol{\chi}(\boldsymbol{x}, t_{n+1}; t), t) \\ \boldsymbol{\chi}(\boldsymbol{x}, t_{n+1}; t_{n+1}) &= \boldsymbol{x} \end{aligned}$$

To compute the $\tilde{\boldsymbol{u}}^{n+1-q}$, the natural approach is then to use the "method of characteristics", i.e. to determine for each mesh-point $\boldsymbol{x}_k$ the value of the velocity $\boldsymbol{u}$ at the time-steps $\{t_n, t_{n-1}, .., t_{n+1-Q}\}$ and at the points $\boldsymbol{\chi}(\boldsymbol{x}_k, t_{n+1}; t_{n+1-q})$, $q = 1, .., Q$. The main drawback is then that the spatial interpolation must be of low order: A high-order interpolation would be too expensive and moreover would yield instabilities on Gauss-Lobatto grids, as investigated both theoretically and numerically in [12].

The "Operator Integration Factor" (OIF) Semi-Lagrangian method [15, 17, 21] constitutes an alternative to the "method of characteristics". It consists in determining the $\tilde{\boldsymbol{u}}^{n+1-q}$ by solving the Q auxiliary problems :

$$\begin{cases} \partial_t \boldsymbol{\phi} + \boldsymbol{u}.\nabla \boldsymbol{\phi} = 0 \qquad t_{n+1-q} \le t \le t_{n+1} \\ \boldsymbol{\phi}(\boldsymbol{x}, t_{n+1-q}) = \boldsymbol{u}^{n+1-q}(\boldsymbol{x}) \end{cases}$$

Then $\tilde{\boldsymbol{u}}^{n+1-q} = \boldsymbol{\phi}^{n+1}$.

Solving this set of problems constitutes what we call the transport step. The basic idea is to transport the $\boldsymbol{u}^{n+1-q}(\boldsymbol{\chi}(\boldsymbol{x}_k, t_{n+1}; t_{n+1-q}))$ at the mesh points, so that interpolations / extrapolations are only needed in time (for $\boldsymbol{u}$). Moreover, the auxiliary problems may be solved by using an explicit scheme with large absolute stability region (e.g. the RK4 scheme) with, if necessary, sub-time cycling.

2.2. Diffusion step. At each time t_{n+1} one computes in the diffusion step a provisional velocity which solves:

$$\begin{aligned} (\frac{1}{Re}\nabla^2 - \frac{\alpha_0}{\Delta t})\,\boldsymbol{u}^* &= \boldsymbol{f}^{n+1} \quad in\,\Omega \\ +B.C., \quad e.g. \quad \boldsymbol{u}^*|_\Gamma &= \boldsymbol{u}^{n+1}|_\Gamma = \boldsymbol{u}_\Gamma \end{aligned}$$

where :

$$\boldsymbol{f}^{n+1} = \frac{1}{\Delta t} \sum_{q=1}^{q=Q} \alpha_q \tilde{\boldsymbol{u}}^{n+1-q} + \nabla p^*$$

with p^* a provisional pressure. In the frame of a second order implementation: $Q = 2$ and $p^* = p^n$ ("Goda scheme").

Note that a similar elliptic but scalar equation is solved for the temperature.

2.3. Projection step. The goal is here to compute a divergence-free velocity field. To this end we solve the *Darcy problem*:

$$\begin{aligned} \boldsymbol{u}^{n+1} + \nabla\varphi &= \boldsymbol{u}^* \quad in\,\Omega \\ \nabla \cdot \boldsymbol{u}^{n+1} &= 0 \quad in\,\Omega \\ \boldsymbol{u}^{n+1} \cdot \boldsymbol{n}|_\Gamma &= \boldsymbol{u}_\Gamma \cdot \boldsymbol{n} \end{aligned}$$

and then update the pressure field $p^{n+1} = p^n + \alpha_0\varphi/\Delta t$.

Solving the above Darcy problem is not straightforward. Following [1, 3] we use a *unique grid* $P_N - P_{N-2}$ strategy (2D case). Thus, let us assume that $\Omega = (-1, 1)^2$ and denote by: (i) P_N, the space of the polynomials of maximum degree N_1 in x and N_2 in y, i.e. $N = (N_1, N_2)$, (ii) Ω_N (Γ_N), the inner (boundary) Chebyshev Gauss-Lobatto collocation points. Then, when using a *Collocation method* we are led to solve the following discrete problem:

Find $\boldsymbol{u}_N \in P_N^2$ and $\varphi_{N-2} \in P_{N-2}$, where $N - 2 = (N_1 - 2, N_2 - 2)$, such that:

$$\begin{aligned} \boldsymbol{u}_N + \nabla\varphi_{N-2} &= \boldsymbol{u}_N^* \quad in\,\Omega_N \\ \nabla \cdot \boldsymbol{u}_N &= 0 \quad in\,\Omega_N \\ \boldsymbol{u}_N \cdot \boldsymbol{n} &= \boldsymbol{u}_\Gamma \cdot \boldsymbol{n} \quad on\,\Gamma_N \end{aligned}$$

This problem can be exactly solved by considering the following *pseudo-Poisson* problem for φ:

$$\begin{aligned} \nabla^2\varphi_{N-2} &= \nabla \cdot \boldsymbol{u}_N^* + \nabla \cdot \boldsymbol{\tau}_N \quad in\,\Omega_N \\ \boldsymbol{\tau}_N &= 0 \quad in\,\Omega_N \\ \partial_n\varphi_{N-2} &= \boldsymbol{\tau}_N \cdot \boldsymbol{n} \quad on\,\Gamma_N, \end{aligned}$$

where $\boldsymbol{\tau}_N$ is nothing but the residual polynomial which results from the fact that the equations are not enforced at the boundary points.

The above formulation holds in the one domain case. In the frame of our unidimensional domain decomposition, there are S subdomains in the streamwise x-direction. In order to enforce the natural C^1 continuity of the pressure at the subdomain-interfaces we use, in each subdomain Ω^s, the pressure polynomial space $P_{N'}(\Omega^s)$ such that:

$s = 1$ or $s = S$	$1 < s < S$
$N' = (N_1 - 1, N_2 - 2)$	$N' = (N_1, N_2 - 2)$

In the 3D case with one homogeneous direction, using the Fourier expansion of each variable the 3D problem splits into a set of 2D-like problems.

3. From DNS to LES. When turbulent flows are concerned, DNS approaches generally fail and so one must go to statistical approaches or to large eddy simulation. Here we show how the numerical method described in Section 2 may be modified to handle turbulent flows. Especially we are going to focus on a defiltering - transport - filtering (DTF) algorithm that we introduced in [16]. Such an algorithm makes use of a stabilization technique, the spectral vanishing viscosity (SVV) method, which may also be used alone to compute high-Reynolds number flows.

3.1. LES equations and the closure problem. For the LES of incompressible flows one has to consider the filtered incompressible Navier-Stokes equations:

$$\begin{cases} \partial_t \bar{\boldsymbol{u}} + \nabla \cdot (\bar{\boldsymbol{u}} \otimes \bar{\boldsymbol{u}}) = -\nabla \bar{p} + \nu \nabla^2 \bar{\boldsymbol{u}} - \nabla \cdot \tau \\ \nabla \cdot \bar{\boldsymbol{u}} = 0 \end{cases}$$

with $\bar{\boldsymbol{u}} = (\bar{u}_1, \bar{u}_2, \bar{u}_3)$ and $\bar{p}$ the filtered velocity and "pressure" respectively:

$$\bar{u}_i = G u_i \quad \textit{and} \quad \bar{p} = G p$$

where G is a convolution operator based on a filter function g of filter width Δ and with τ the "sub-grid-scale" stress (SGS) tensor:

$$\tau_{ij} = \overline{u_i u_j} - \bar{u}_i \bar{u}_j$$

Then occurs a closure problem, since the SGS tensor must be modeled.

One possible closure is offered by the Velocity estimation models or Approximate Deconvolution Method (ADM) [6, 18, 19] which expresses the SGS tensor as:

$$\tau_{ij} = \overline{G^+ \bar{u}_i G^+ \bar{u}_j} - \overline{G^+ \bar{u}_i}\ \overline{G^+ \bar{u}_j}$$

where G^+ is an approximate inverse of G ("defiltering operator"). Note that with $G^+ = 1$ one recovers the *Scale similarity model* [2].

Such models are known to be not enough dissipative but better on "*a priori* tests" than *Eddy viscosity models*, which state a proportionality between the SGS tensor and the strain rate tensor. To overcome the stability problem, one often uses *mixed models* which make use of both scale similarity and eddy viscosity.

3.2. A no-SGS model approach. Before going farther in the field of LES, let us mention that the computation of turbulent flows can also be achieved by using a stabilization technique. In the frame of spectral methods, the *Spectral vanishing viscosity (SVV) method* [20, 14] is specially of interest, because it allows to enforce the scheme stability while preserving the spectral accuracy.

The SVV method was first developed for the non-linear conservation law :

$$\partial_t u + \partial_x (f(u)) = 0$$

for which one solves:

$$\partial_t u_N + \partial_x I_N(f(u_N)) = \epsilon_N \partial_x (Q(\partial_x u_N))$$

with $\epsilon_N = O(1/N)$ and where I_N denotes the polynomial interpolation onto P_N and Q the spectral viscosity operator such that (L_k: Legendre polynomial of degree k):

$$Q\phi \equiv \sum_{k=0}^{N} \hat{Q}_k \hat{\phi}_k L_k, \quad \forall \phi, \quad \phi = \sum_{k=0}^{N} \hat{\phi}_k L_k$$

with: $\hat{Q}_k = 0$ if $k \leq m_N$ and $1 \geq \hat{Q}_k \geq 1 - (m_N/k)^4$ if $k > m_N$, $m_N = O(\sqrt{N})$.

The no-model approach suggested here was e.g. used in [10].

3.3. DTF (Defiltering-Transport-Filtering) algorithm. The basic idea is to combine (i) the ADM and (ii) the OIF "semi-Lagrangian method" described in Section 2. In convective form the filtered Navier-Stokes equations read:

$$\begin{cases} \overline{D_t \boldsymbol{u}} = -\nabla \bar{p} + \nu \nabla^2 \bar{\boldsymbol{u}}, \\ \nabla \cdot \bar{\boldsymbol{u}} = 0. \end{cases}$$

From the approximation of the material derivative introduced in Section 2 (BEQ scheme) one obtains:

$$\overline{D_t \boldsymbol{u}} \approx \frac{1}{\Delta t}(\alpha_0 \bar{\boldsymbol{u}}^{n+1} + \sum_{q=1}^{q=Q} \alpha_q \bar{\tilde{\boldsymbol{u}}}^{n+1-q}).$$

Then the closure problem consists in determining the $\bar{\tilde{\boldsymbol{u}}}^{n+1-q}$ from the $\bar{\boldsymbol{u}}^{n+1-q}$. In [16] it is suggested to use:

$$\bar{\tilde{\boldsymbol{u}}}^{n+1-q} = (1 + G\,(T-1)\,G^{+})\bar{\boldsymbol{u}}^{n+1-q}$$

where $T(\boldsymbol{u})$ stands for the transport operator such that $\tilde{\boldsymbol{u}}^{n+1-q} = T\boldsymbol{u}^{n+1-q}$. Note that the straightforward approach:

$$\bar{\tilde{\boldsymbol{u}}}^{n+1-q} = G\,T\,G^{+}\bar{\boldsymbol{u}}^{n+1-q}$$

yields a non-consistent algorithm, because in the limit $\Delta t = 0$, for which $T = 1$, we have $GG^{+} \neq 1$ (G^{+} is indeed only an approximate inverse of G).

As it stands, the DTF algorithm is of ADM type, which means that being not enough dissipative it must be associated with a stabilization technique, just like the mixed models which combine scale similarity and eddy viscosity [5]. To this end, we will use the SVV method, which shows the essential property to preserve the spectral accuracy of the approximation.

3.4. Choice of the filtering and defiltering operators. As developed in [11] one can use Taylor expansions of the u_i to get approximations of the Gaussian (or "box") filter and of its inverse and thus set up the filtering and defiltering operators. Indeed, with a four'th order approximation (regular grid) :

$$G = 1 + A \quad \textit{and} \quad G^{+} = 1 - A,$$

where $A = \frac{1}{24}\sum_{i=1}^{3} \Delta_i^2 \partial_i^2$, with Δ_i the space step size in i-direction.

However, as explained in [16], in the frame of spectral methods such an approach fails due to the fact that the treatment of the highest frequencies is not adequate. Nevertheless, keeping in mind the basic idea one can develop a filtering approach in spectral space which effectively shows the properties of an usual filter and moreover opens a way toward a two-level grid approach. The spectrum of the proposed filter, G', is shown in Fig. 3.1. It is essentially the one of G, but vanishes beyond a critical wavenumber, say k_c. Using such a filter is in fact close to using a two-level grid approach, as promoted e.g. in [4], since at $k = k_c$ is implicitely associated a coarse grid. Roughly speaking, the computational grid is then only fully used in the transport step where the closure problem is handled.

For both the Fourier and Chebyshev approximations such a filter directly acts on the Fourier or Chebyshev spectra. In case of the Chebyshev approximation this corresponds to apply a filter of constant width to the 2π-periodic function $u(-\cos(z)), z \in R$.

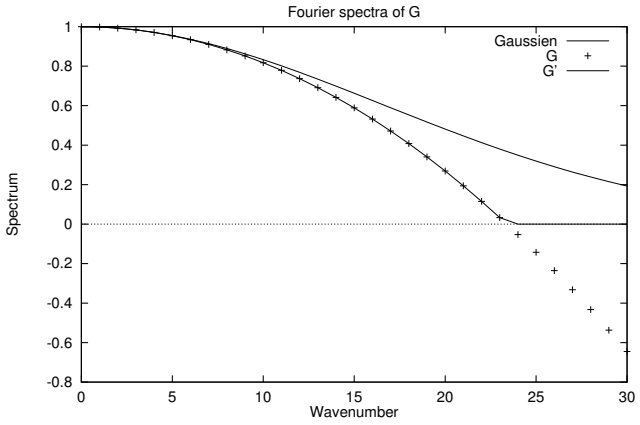

FIG. 3.1. *Spectra of the Gaussian filter and of its approximations G and G'. The (non-plotted) spectrum of G^+ is symmetric to the one of G*

4. Applications. First, we present results obtained for the wake of a sphere in a stratified liquid (our early results were presented in [8]). The influence of the stratification is pointed out by considering two different values of the Richardson number, $Ri = 0$ and $Ri = 0.25$. In case $Ri = 0$, the temperature behaves as a passive scalar. Second we compute the turbulent wake of a cylinder and compare results obtained with the SVV method and the DTF algorithm combined with the SVV.

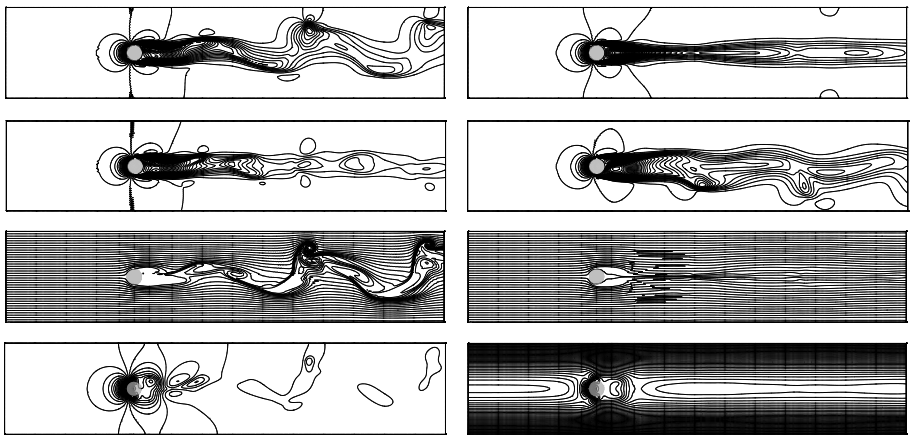

FIG. 4.1. *Streamwise velocity (front and top views), temperature and pressure (front view) for $Ri = 0$ (left) and $Ri = 0.25$ (right)*

4.1. Wake of a sphere in a stratified liquid. Computations have been carried out with: Control parameters: $Re = 300$ (based on the diameter and on the mean flow velocity), $Ri = \{0, 0.25\}$ (corresponding internal Froude number $F = \{\infty, 2\}$); Initial conditions: constant temperature gradient, fluid at rest; Boundary conditions: Dirichlet at the inlet, homogeneous Neumann for T and free-slip for $\boldsymbol{u}$ at the horizontal boundaries, soft OBC at the outlet; Computational domain: $\Omega =]0, 29[\times]-3, 3[\times]0, 6[$, sphere of unit diameter centered at $(8.5, 0, 3)$; Spatial and temporal approximations:

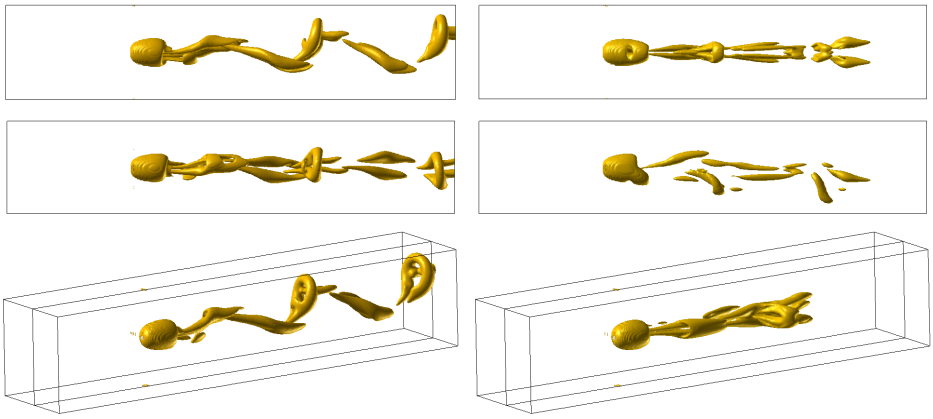

FIG. 4.2. *Vortical structures (Q criterion), front, top and perspective views for* $Ri = 0$ *(left) and* $Ri = 0.25$ *(right)*

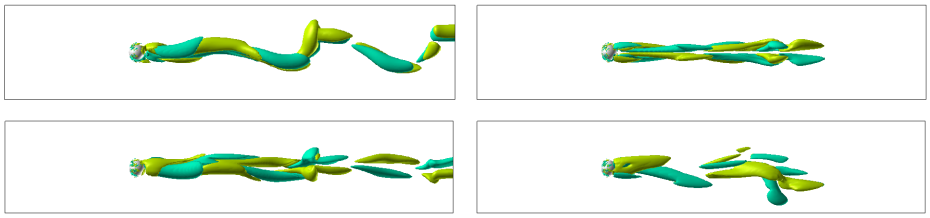

FIG. 4.3. $\omega_x = \pm 0.2$, *front and top views for* $Ri = 0$ *(left) and* $Ri = 0.25$ *(right)*

$S = 16$, $N_1 = 30$, $N_2 = 90$, number of Fourier grid-points $N_F = 90$, $\Delta t = 10^{-2}$, no sub-cycling in the transport step.

In Fig. 4.1 are shown isolines of the streamwise velocity, of the temperature and of the pressure for the two values of the Richardson number. Clearly one observes the confinement effect (streamwise velocity) and the blocking effect (temperature) of the stratification when it is active, i.e for $Ri = 0.25$. One notices that the pressure fields are completely different. This results from the fact that for $Ri = 0.25$ one essentially observes the background parabolic pressure field associated with the constant temperature gradient.

Using the Q criterion (see e.g. [9]) the vortical structures are visualized in Fig. 4.2. Here again, the confinement effect is clearly visible. Moreover, one can discern some horse-shoe type structures typically encountered for such wakes.

In Fig. 4.3 is visualized the streamwise component of the vorticity, which is the relevant variable to understand the snake-like deformation of the wake. In a $y - z$ plane one can indeed discern two pairs of contra-rotating cells. Their effects cancel each-other at the "nodes" of the wake whereas between them one contra-rotating cell is dominating and so induces the deformation of the wake.

4.2. Wake of a cylinder. The calculations are characterized by: Control parameters: $Re = 3900$ (based on the diameter and on the mean flow velocity), see e.g. [13], $Ri = 0$; Initial and boundary conditions: same as those used in previous subsection; Computational domain: $\Omega = (-6.5, 17.5) \times (-4, 4) \times (0, 4)$, cylinder of unit diameter with axis at $x = y = 0$. Spatial and temporal approximations: $S = 5$,

$N_1 = 60$, $N_2 = 120$, $N_F = 60$, $\Delta t = 5\,10^{-3}$, no sub-cycling in the transport step. Visualizations at a given time of the strongly 3D flow computed with the SVV

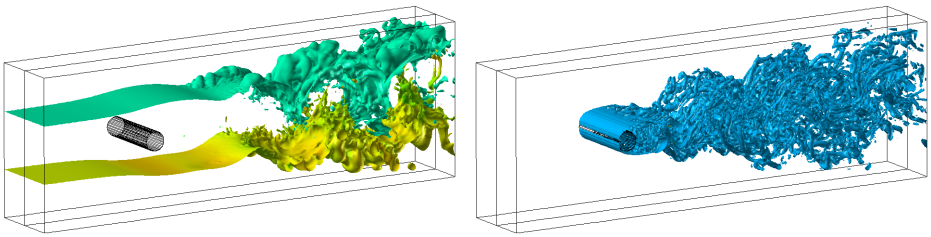

FIG. 4.4. *Isotherms (left) and Q criterion (right) with SVV*

method are shown in Fig. 4.4. At left two isotherms are visualized and at right it is the Q criterion. A qualitative idea of the difference between the results obtained

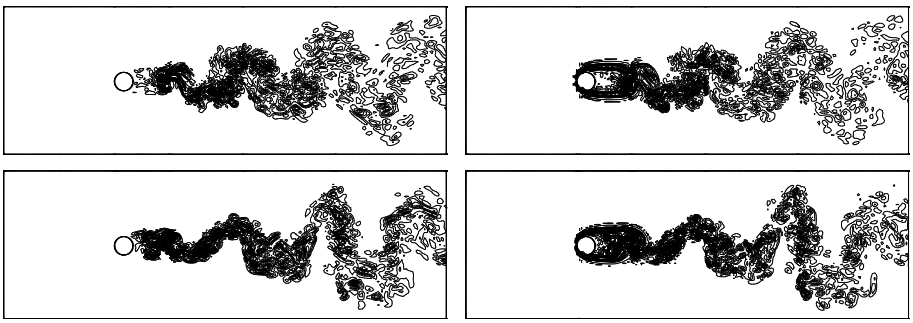

FIG. 4.5. *Streamwise (left) and spanwise (right) components of the vorticity for DTF (top) and SVV (bottom)*

with the SVV and DTF (+SVV for stabilization) approaches may arise from the Fig. 4.5 and 4.6. Fig. 4.5 compares the streamwise and spanwise components of the vorticity, through their isolines in the central vertical plane $z = 2$ and Fig. 4.6 shows front views of the Q criterion. At this qualitative level, the results appear very

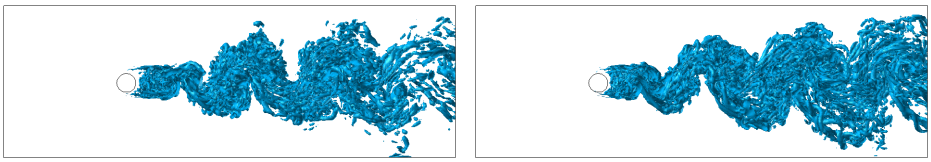

FIG. 4.6. *Q criterion for DTF (left) and SVV (right)*

similar. More detailed investigations will be carried out in next future.

Acknowledgments. The computations were made on the NEC-SX5 computer of the IDRIS computational center (project 024055). We are grateful to J.M. Lacroix, engineer of the CNRS, for his helpful contribution.

REFERENCES

[1] M. Azaiez, A. Fikri and G. Labrosse, *A unique grid spectral solver of the nD Cartesian unsteady Stokes system. Illustrative numerical results*, in Finite Elem. Anal. Des., 16, (3-4), (1994), pp. 247–260.

[2] J. Bardina, J.H. Ferziger and W.C. Reynolds, *Improved turbulence models based on large eddy simulation of homogeneous incompressible turbulence*, Stanford University, Report TF-19 (1983).

[3] O. Botella, *On the solution of the Navier-Stokes equations using Chebyshev projection schema with third order accuracy in time*, in Computers & Fluids, 26 (2), (1997) pp. 107–116.

[4] J.A. Domaradzki and E.M. Saiki, *A subgrid-scale model based on the estimation of unresolved scales of turbulence*, in Phys. Fluids, 9 (7), (1997), pp. 2148–2164.

[5] T.B. Gatsky, M.Y. Hussaini and J.L. Lumley, *Simulation and modeling of turbulent flows*, in ICASE/LaRC Series in Computational Science and Engineering, Chapter 3, Large Eddy Simulation, by J.H. Ferziger, (1996) pp. 109–154.

[6] B.J. Geurt, *Inverse modeling for large-eddy simulation*, in Phys. Fluids, 9 (12), (1997), pp. 3585–3587.

[7] M.Y. Forestier, R. Pasquetti, R. Peyret and C. Sabbah, *Spatial development of wakes using a spectral multi-domain method*, in Applied Numerical Mathematics, 33, (2000), pp. 207–216.

[8] M.Y. Forestier, R. Pasquetti and R. Peyret, *Computations of 3D wakes in stratified fluids*, Computational Fluid Dynamics Conference ECCOMAS 2000, (2000), proc. in CD.

[9] J. Jeong and F. Hussain, *On the identification of a vortex*, in J. Fluid Mech., 285, (1995), pp. 69–94.

[10] G.S. Karamanos and G.E. Karniadakis, *A spectral vanishing viscosity method for large-eddy simulation*, in J. Comput. Phys., 163, (2000), pp. 22–50.

[11] F.V. Katopodes, R.L. Street and J.H. Ferziger, *A theory for the subfilter-scale model in large-eddy simulation*, Stanford University, Tech. Report 2000-K1 (2000).

[12] S. Kraütle, *A Navier-Stokes solver based on CGBI and the method of characteristics*, Phd thesis, Erlangen University (2002).

[13] A.G. Kravchenko and P. Moin, *Numerical studies of flow over a circular cylinder at Re=3900*, in Phys.Fluids, 12 (2), (2000), pp. 403–417.

[14] Y. Maday, S.M.O. Kaber and E. Tadmor, *Legendre pseudo-spectral viscosity method for nonlinear conservation laws*, in SIAM J. Numer. Anal., 30 (2), (1993), pp. 321–342.

[15] Y. Maday, A.T. Patera and E.M. Ronquist, *An operator-integration-factor splitting method for time-dependent problems: application to incompressible fluid flow*, in J.of Sci. Comp., 5 (4), (1990), pp. 263–292.

[16] R. Pasquetti and C.J. Xu, *High-order algorithms for large eddy simulation of incompressible flows*, in J. Sci. Comp., 17 (1-4), (2002), pp. 273–284.

[17] R.M. Phillips and T.N. Phillips, *Flow past a cylinder using a semi-Lagrangian spectral element method*, in Appl. Num. Math, 33, (2000), pp. 251–257.

[18] S. Stolz and N.A. Adams, *An approximate deconvolution procedure for large-eddy simulation*, in Phys.Fluids, 11 (7), (1999), pp. 1699–1701.

[19] S. Stolz, N.A. Adams and L. Kleiser, *An approximate deconvolution model for large-eddy simulation with application to incompressible wall-bounded flows*, in Phys.Fluids, 13 (4), (2001), pp. 997–1015.

[20] E. Tadmor, *Convergence of spectral methods for nonlinear conservation laws*, in SIAM J. Numer. Anal., 26 (1), (1989), pp. 30–44.

[21] C.J. Xu and R. Pasquetti, *On the efficiency of semi-implicit and semi-Lagrangian spectral methods for the calculation of incompressible flows*, in Inter. J. Numer. Meth. Fluids, 35, (2001), pp. 319–340.